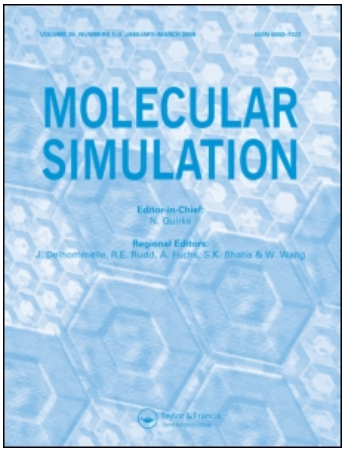

Molecular Simulation
Publication details, including instructions for authors and subscription information:
http://www.informaworld.com/smpp/title~content=t713644482

Diffusive Dynamics in a Detailed Potential: Application to Biological Macromolecules

Simone Fausti[ab]; Giovanni La Penna[a]; Carla Cuniberti[b]; Angelo Perico[a]
[a] Istituto di Studi Chimico-Fisici di Macromolecole Sintetiche e Naturali, National Research Council, Genova, Italy [b] Dipartimento di Chimica e Chimica Industiale, Università di Genova, Genova, Italy

To cite this Article Fausti, Simone , La Penna, Giovanni , Cuniberti, Carla and Perico, Angelo(2000) 'Diffusive Dynamics in a Detailed Potential: Application to Biological Macromolecules', Molecular Simulation, 24: 4, 307 — 324
To link to this Article: DOI: 10.1080/08927020008022378
URL: http://dx.doi.org/10.1080/08927020008022378

Molecular Simulation, 2000, Vol. 24, pp. 307–324
Reprints available directly from the publisher
Photocopying permitted by license only

DIFFUSIVE DYNAMICS IN A DETAILED POTENTIAL: APPLICATION TO BIOLOGICAL MACROMOLECULES

SIMONE FAUSTI[a,b], GIOVANNI LA PENNA[a], CARLA CUNIBERTI[b] and ANGELO PERICO[a,*]

[a]*Istituto di Studi Chimico-Fisici di Macromolecole Sintetiche e Naturali, National Research Council, Via De Marini 6, 16149 Genova, Italy;*
[b]*Dipartimento di Chimica e Chimica Industiale, Università di Genova, Via Dodecaneso 31, 16146 Genova, Italy*

(Received April 1999; accepted May 1999)

The local dynamics of macromolecules is obtained to second-order in the mode-coupling expansion of the Smoluchowski diffusion theory. The NMR spin-lattice relaxation times of different ^{13}C or ^{15}N nuclei along the chains are calculated and compared to experimental data from the literature. The macromolecules are considered as fluctuating 3D structures undergoing rotational diffusion. The fluctuations can be evaluated with any technique for sampling the configurational space. In the presented test cases Molecular Dynamics simulations have been applied to a DNA fragment and to the NK-2 homeodomain. In the case of the double-stranded DNA fragment $d(TpCpGpCpG)_2$, second and even first order theories are found to be in close agreement with experimental results. The major advantage of the diffusion technique is that only a good statistics is important as input while the solvent dynamic effects enter through hydrodynamic theory. Application based on Hybrid Monte Carlo schemes coupled with J-walking, are now in progress.

Keywords: Diffusive dynamics; biological macromolecules

1. INTRODUCTION

In recent years, increasing attention has been devoted to the study of the macromolecules local dynamics. Such big molecules permit different domains, of different mobility, to be on the same units. These local

*Corresponding author.

flexibilities may play a significant role in most of biological processes (*i.e.*, molecular recognition). Experimentally, spin-lattice ^{13}C-NMR relaxation data are currently analysed using empirical methods such as the popular Lipari and Szabo equation (Lipari, 1984) to investigate local dynamics.

The approach, we are now going to explain, can be also a new method to analyse NMR data, but is principally a self-standing theory that can be later constructively compared with the experiments. Starting from the Smoluchowski equation describing the time evolution of the atomic coordinate diffusing in an empirical intramolecular potential, we find solutions with different approximations.

The diffusion theory initially ignores the memory functions, producing the optimized Rouse-Zimm approximation (Bixon, 1978); by means of a mode-coupling approach the memory function effects are evaluated for one-dimensional systems without hydrodynamic interactions (Perico, 1993; Perico, 1994). Recently the above approach has been extended to multidimensional systems with hydrodynamic interactions, as necessary for complex molecules (Perico, 1997). In this framework the dynamics of stiff synthetic and biological macromolecules, such as proteins and DNA double helices, may be described as the diffusion of fluctuating three-dimensional structures (Perico, 1995). For these systems the rotational dynamics of the rigid three-dimensional structure represent a first natural model approximation and also the main contribution to the local dynamics of the fluctuating chain. Taking the fluctuations into account by averaging over a statistics of conformations (*i.e.*, a MD trajectory), we collect inputs for the proposed theory (La Penna, 1999).

We discuss here some recent applications for proteins (NK-2 homeodomain (La Penna, 1999*)) and oligonucleotides, in particular the DNA-fragment d(TpCpGpCpG)$_2$ (Fausti, 1999) is considered because NMR data are available from the literature (Borer, 1994).

2. THE MODE-COUPLING EXPANSION SOLUTION OF SMOLUCHOWSKI DYNAMICS

Here we summarize the mode-coupling diffusion approach to dynamics in polymer solutions (Perico, 1997; La Penna, 1999). Given a polymer of N_a beads with friction coefficients ζ_i and coordinates $\mathbf{r}_i$, $i = 1, \ldots, N_a$, the dynamics of bond vectors connecting two beads, $\mathbf{l}_j, j = 1, \ldots, N_b$, is governed by the Smoluchowski operator L, the adjoint operator to the diffusion

operator D, such that

$$\frac{\partial}{\partial t}\mathbf{l} = L\mathbf{l} \tag{1}$$

where

$$L = \sum_{i,j=1}^{N_a} [\nabla_i \cdot \mathbf{D}_{ij} \cdot \nabla_j - (\nabla_i U/k_B T) \cdot \mathbf{D}_{ij} \cdot \nabla_j] \tag{2}$$

and $\mathbf{l}$ is the $3N_b$-dimensional array with the coordinates of the bond vectors.

Here the diffusion tensor is given by

$$\mathbf{D}_{ij} = D_i \mathbf{H}_{ij} \tag{3}$$

The $\mathbf{D}$ operator is, therefore, defined in terms of the factors D_i and $\mathbf{H}_{ij}$:

$$\mathbf{H}_{ij} = \mathbf{1}\delta_{ij} + \frac{\zeta_r'}{\zeta_r}\zeta_i \mathbf{T}_{ij}(1 - \delta_{ij}), \tag{4}$$

$$\mathbf{T}_{ij} = (8\pi\eta r_{ij})^{-1}[\mathbf{1} + \mathbf{r}_{ij}\mathbf{r}_{ij}/r_{ij}^2] \tag{5}$$

where $\mathbf{H}$ and $\mathbf{T}$ represent the hydrodynamic interaction matrix and Oseen tensor, respectively, and

$$D_i = k_B T/\zeta_i \tag{6}$$

where D_i is the diffusion coefficient of bead i. U is the intramolecular potential, and η is the solvent viscosity.

The factor ζ_r'/ζ_r before the hydrodynamic interaction is a parameter whose values are restricted to the range $0 < \zeta_r' < 0.6$ to maintain a positive definite $\mathbf{H}$. In the case of the DNA oligomer we fix ζ_r' at the standard value 0.25 (Perico, 1975), while in other cases, for instance the NK-2 homeodomain, different values have been tested with different representations of hydrodynamics (*i.e.*, Rotne and Prager form). The meaning of the above parameters is here summarised:

$$\zeta_r = \zeta/6\pi\eta l, \tag{7}$$

ζ being the average friction coefficient

$$\zeta = \frac{1}{N_a}\sum_{i=1}^{N_a}\zeta_i \tag{8}$$

and l the root mean square bond length

$$l^2 = \frac{1}{N_b}\sum_{i=1}^{N_b}\langle l_i^2\rangle \tag{9}$$

By expanding the conditional probability (solution of the Smoluchowski equation) in a complete set of eigenfunctions of L, the time autocorrelation function (TCF) of any dynamic variable with zero average $f(\mathbf{l})$ may be expressed in the standard form

$$\langle f(t)f(0)\rangle = \sum_i \langle f|\psi_i\rangle\langle\psi_i|f\rangle \exp(-\lambda_i t), \tag{10}$$

where λ_i and ψ_i are the eigenvalues and the normalized eigenfunctions of the operator L

$$L\psi_i = -\lambda_i\psi_i. \tag{11}$$

The matrix expansion method for the calculation of the TCF $\langle f(t)f(0)\rangle$ requires solution of the eigenvalue problem in Eq. (11) by expanding ψ_i in a set of basis functions $\Phi = \{\phi_m, m = 1, \ldots, M\}$,

$$\psi_i = \sum_{m=1}^{M} C_{m,i}\phi_m \tag{12}$$

thus converting Eq. (11) into the generalized matrix eigenvalue equation

$$\mathbf{FC} = \mathbf{SC\Lambda}, \tag{13}$$

with $\mathbf{\Lambda}$ the diagonal matrix of the eigenvalues λ_m, $\mathbf{C}$ the eigenvector matrix of coefficients $C_{i,m}$, $\mathbf{S}$ the metric matrix

$$S_{ij} = \langle\phi_i|\phi_j\rangle, \tag{14}$$

and $\mathbf{F}$ the equilibrium force matrix

$$F_{ij} = -\langle\phi_i|L\phi_j\rangle = \sum_{m,n=1}^{N_a}\langle(\nabla_m\phi_i)\cdot\mathbf{D}_{mn}\cdot(\nabla_n\phi_j)\rangle. \tag{15}$$

The ensemble equilibrium averages, indicated within brackets in the above equations, are calculated as

$$\langle a|b\rangle = \int P_{\mathrm{eq}}(\mathbf{r})a(\mathbf{r})b(\mathbf{r})d\mathbf{r}, \tag{16}$$

with $P_{eq}(\mathbf{r})$ being the equilibrium distribution function. As the eigenfunctions ψ_i are orthonormalized, the coefficient matrix $\mathbf{C}$ should satisfy the normalization equation

$$\mathbf{C}^T\mathbf{S}\mathbf{C} = \mathbf{1}. \tag{17}$$

Given a basis set, the dynamics are derived by solving Eq. (13). Note that in the general case of a fluctuating molecule, the matrix $\mathbf{S}$ is non-singular and Eq. (13) is solved as

$$\mathbf{S}^{-1}\mathbf{F}\mathbf{C} = \mathbf{C}\Lambda, \tag{18}$$

while in the case of a rigid structure, $\mathbf{S}$ is highly singular and the dynamics problem may still be solved by inverting Eq. (13) to

$$\mathbf{F}^{-1}\mathbf{S}\mathbf{C} = \mathbf{C}\Lambda^{-1} \tag{19}$$

which has the same eigenvectors and inverse eigenvalues.

Accurate approximations of the evaluation of TCFs are obtained by considering increasing powers of the variables (bond vectors or their combinations) in the spirit of the mode-coupling theory (La Penna, 1999; Kostov, 1997; Perico, 1997).

Autocorrelation functions obtainable, for instance, by dielectric, fluorescence, Raman and Nuclear Magnetic Resonance experiments are of the form:

$$P_L(t) = \langle P_L(\cos(\beta(t)))\rangle = \sum_{M=-L}^{L} \left\langle D_{M,0}^{(L)^*}(\Omega(t)) D_{M,0}^{(L)}(\Omega(0))\right\rangle \tag{20}$$

where P_L is the Legendre polynomial of order L, β is the angle that a given vector spans in the time t, and the average is over all the possible choices of time origins (*i.e.*, over the equilibrium distribution of orientations) and over the equivalent vectors in the sample. The functions $D_{M,N}^{(L)}$ are Wigner matrix elements and $D_{M,0}^{(L)}$ are irreducible spherical tensors (Rose, 1957).

As f is an L-rank irreducible spherical function of a molecular vector, the projections $\langle f|\phi_m\rangle$ on the basis elements ϕ_m required in Eq. (10) are non-zero if and only if ϕ_m is an L-rank function. Therefore, the ϕ_m basis functions must be constructed as L-rank functions. As a consequence, the $\mathbf{S}$ and $\mathbf{F}$ matrix elements are averages of products of L-rank irreducible spherical tensors. The evaluation of these elements is done simply by computing the scalar components (rotational invariants) contained in the products of L-rank functions in the matrix elements (La Penna, 1999).

We outline below an efficient procedure for finding a reduced basis set to compute accurate tensor time correlation functions; this is derived by extension of a similar calculation performed in the case of rigid 3D structures (La Penna, 1999). The first step amounts to solving the diffusion equation with a basis that is linear in the bonds in order to get the first order P_1 dynamics:

$$\{l_{i,x}\} \quad i = 1, \ldots, N_b \tag{21}$$

This basis can be used to derive the TCF

$$M_1^{(l)}(t) = \frac{\langle \mathbf{l}(t) \bullet \mathbf{l}(0) \rangle}{\langle \mathbf{l} \bullet \mathbf{l} \rangle} \tag{22}$$

and in turn, through an analytic relation, the first order ORZLD solution to $P_2^{(l)}(t)$ (Perico, 1985), which will be used in Section 5.

The first order solution is obtained by diagonalization of Eq. (18), which gives the first order P_1 eigenfunctions $m_{i,x}$:

$$m_{i,x} = \sum_{j=1}^{N_b} C_{j,i} l_{j,x}. \tag{23}$$

These eigenfunctions may be considered as a new basis set equivalent to the bond basis set in Eq. (21), giving identical results for the eigenvalues, which are the mode relaxation rates, and for TCFs.

For a rigid structure in d dimensions, only d eigenvalues are non-infinite, and the TCF in Eq. (22) has only d exponential contributions. The full mode basis set of N_b elements in Eq. (23) can be substituted with a reduced first order P_1 basis set of only d elements, the modes corresponding to non-infinite relaxation rates. In the case of fluctuating rigid structures, the first d modes of lower relaxation rate correspond to eigenvalues clearly separated from the rates of the higher modes (which are found to be greater than two orders of magnitude). Therefore we can select a reduced basis set, generally built with the e modes of Eq. (23) of lowest rates, with e equal to d or a value much lower than N_b.

For quasi-rigid structures, ignoring the modes of higher rates means ignoring very small contributions to the TCFs corresponding to fast decaying exponential terms related to these modes. This is evident at the first order and is still valid at higher orders due to the combined effect of the products of fast decaying exponential terms.

For 2-rank functions, a reduced first order basis set can be taken in the form:

$$\Phi_I^{(2)} = \left\{\phi_{i,M}^{(2)}\right\} \quad \text{(RM2 - I)} \tag{24}$$

where

$$\begin{aligned}
\phi_{i,0}^{(2)} &= \frac{1}{2}\,(3m_{i1,z}m_{i2,z} - \mathbf{m}_{i1}\cdot\mathbf{m}_{i2}) \\
\phi_{i,-2}^{(2)} &= \sqrt{\frac{3}{8}}\,(m_{i1,x}m_{i2,x} - m_{i1,y}m_{i2,y}) \\
\phi_{i,2}^{(2)} &= \sqrt{\frac{3}{8}}\,(m_{i1,x}m_{i2,y} + m_{i1,y}m_{i2,x}) \\
\phi_{i,-1}^{(2)} &= \sqrt{\frac{3}{8}}\,(m_{i1,x}m_{i2,z} + m_{i1,z}m_{i2,x}) \\
\phi_{i,1}^{(2)} &= \sqrt{\frac{3}{8}}\,(m_{i1,y}m_{i2,z} + m_{i1,z}m_{i2,y}) \quad i_1 = 1,\ldots,e;\ i_1 \le i_2
\end{aligned} \tag{25}$$

This is the reduced first order basis set for the P_2 dynamics, and the functions are second powers of the reduced first order P_1 modes. The reduced second order basis set for 2-rank TCFs is built by adding to the first order basis set in Eq. (24) products of the first order basis functions and scalar functions of the vector modes:

$$\Phi_{II}^{(2)} = \Phi_I^{(2)} \cup \left\{\phi_{i,M}^{(2)}\right\} \quad \text{(RM2 - II)} \tag{26}$$

where

$$\begin{aligned}
\phi_{i,0}^{(2)} &= \frac{1}{2}\,(3m_{i1,z}m_{i2,z} - \mathbf{m}_{i1}\cdot\mathbf{m}_{i2})(\mathbf{m}_{i3}\cdot\mathbf{m}_{i4}) \\
\phi_{i,-2}^{(2)} &= \sqrt{\frac{3}{8}}\,(m_{i1,x}m_{i2,x} - m_{i1,y}m_{i2,y})(\mathbf{m}_{i3}\cdot\mathbf{m}_{i4}) \\
\phi_{i,2}^{(2)} &= \sqrt{\frac{3}{8}}\,(m_{i1,x}m_{i2,y} + m_{i1,y}m_{i2,x})(\mathbf{m}_{i3}\cdot\mathbf{m}_{i4}) \\
\phi_{i,-1}^{(2)} &= \sqrt{\frac{3}{8}}\,(m_{i1,x}m_{i2,z} + m_{i1,z}m_{i2,x})(\mathbf{m}_{i3}\cdot\mathbf{m}_{i4}) \\
\phi_{i,1}^{(2)} &= \sqrt{\frac{3}{8}}\,(m_{i1,y}m_{i2,z} + m_{i1,z}m_{i2,y})(\mathbf{m}_{i3}\cdot\mathbf{m}_{i4}) \\
& \qquad i_1 = 1,\ldots,e;\ \ i_1 \le i_2;\ \ i_3 = 1,\ldots,e;\ \ i_3 \le i_4
\end{aligned} \tag{27}$$

Note that, for simplicity's sake, the same notation has been used for first and second order mode-coupling functions.

These fourth powers in the P_1 modes (and in turn in the bonds) give new basis functions that display the same 2-rank properties as Eq. (24). The resulting basis set in the basic choice $e = d = 3$ for a fluctuating 3D structure has $3 \times 2 + (3 \times 2) \times (3 \times 2) = 42$ elements. As observed elsewhere (La Penna, 1999; Perico, 1997), that this second order basis set RM2-II is expected to represent a good approximation of the dynamics of fluctuating structure because it gives the 'exact' rotational dynamics in the rigid limit.

Given the second rank P_2TCFs, the ^{13}C-nmr T_1 relaxation times can be calculated using the standard equations (Abragam, 1986):

$$T_1^{-1}(\omega) = Q[J(\omega_H - \omega_C) + 3J(\omega_C) + 6J(\omega_H + \omega_C)] + (\delta^2/15)\omega_C^2 J(\omega_C) \tag{28}$$

where

$$Q = \frac{n}{20}\left(\frac{1}{4\pi\varepsilon_0 C^2}\frac{\gamma_C\gamma_H\hbar}{r_{CH}^3}\right)^2 \tag{29}$$

n is the number of equivalent protons connected to each observed carbon, γ are the gyromagnetic ratios, r_{CH} is the carbon–proton distance and δ is the chemical shift anisotropy (dimensionless) of the observed nucleus. The first three contributions to the longitudinal relaxation come from the dipolar mechanism, and are present for all the observed nuclei with bonded hydrogen atoms, while the fourth contribution comes from the chemical shift anisotropy fluctuation and will be considered for the aromatic carbons only (C6 in Tymine and Cytosine, C8 in Guanine), with $\delta =$ 185 ppm. The same equations can be applied to the study of ^{15}N relaxation with C replaced by N ($\delta = 160$ ppm).

3. MODELLING A MACROMOLECULE

The first step in the mode-coupling diffusion dynamics is the choice of bond variables, the related beads and bead friction coefficients. Different variables can be chosen and their effects on the local dynamics are analysed with the purpose of reducing the number of variables and limiting the computational cost.

When possible, we start to consider a "quasi atomistic" model: each aliphatic (C, CH, CH_2 and CH_3), carbonyl (C=O), heterocyclic N(=N— or —NH—), amino (—NH—, $—NH_2$), hydroxyl (OH), ether or esteric O and PO_2 group is represented as a single bead (see the most detailed model, named side-chain or SC in the next section, for the DNA fragment). By means of structural considerations we group together the previous beads to build a rougher model, for example rigid domains are straightforward represented as single beads. Also the spherical form of the constructed bead is taken into account as a nice factor.

After building the geometrical model, we have to assign a friction coefficient to every bead in the chain: we decide to use stick boundary condition as derived from literature (Kostov, 1993). The Stokes radii a, that are the radii of a sphere with the same surface of the bead, can be calculated by means of two different approach. The first one is the method of the Van der Waals increments, that has been already used from some authors (Hu, 1991), the second ones works computing the Accessible Surface Area (ASA) of the bead (Gaudio, 1992).

In the cases here reported we have measured ASA Surfaces for an ideal probe of zero radius, so that comparisons were possible between models of different detail. We have not seen relevant differences in the local dynamics of different segments using more than four beads per nucleotide in the DNA case. Superpositions of neighbor atoms are taken into account, the smaller accessible surface reducing proportionally the friction coefficient for an important factor.

The bead friction coefficients of the less detailed models are computed by summing the squares of the friction coefficients over the constituent subunits of that bead and then taking the root square of this number (Zimm method (Kostov, 1993)).

In all the DNA models, the bonds chosen as the first order basis set must exclude one of the bonds in the rings (sugar or base) in order to keep **F** non-singular, but a virtual bond should be present connecting the two strands in order to maintain the agreement between the exact solution and the second order approximated solution for a rigid body: we have always chosen a bond connecting the closest beads in the C2-G10 base pair. This bond is not included in the calculation of the hydrodynamic strength.

Results here reported consider the most detailed model (SC) for the DNA fragment and a virtual bond model for the NK-2 homeodomain, the last one obtained collecting all the beads from SC model for every residue.

4. MOLECULAR STATISTICS

Every method able to sample the statistics of macromolecules in condensed phases can be applied in the calculation of the averages needed to solve the diffusion equation. Molecular Dynamics simulation is particularly suitable for biological molecules in explicit water because the structural effects of water and the high cooperativity between bonds requires the computation of forces and deterministic time evolution of atom positions (Frenkel, 1996). Other techniques are based on the construction of energy maps (Mattice, 1994) and Monte Carlo methods. Among the latter algorithms, the Hybrid Monte Carlo (HMC) algorithm (Duane, 1987) is expected to be suitable for biological molecules since it keeps the advantages of MD and it allows the coupling of thermal MD configurational movements with configurational jumps (J-walking) (Zhou, 1997).

The results reported here are related to application of MD simulations, using the ORAC 3.0 program (Procacci, 1996) and the AMBER 4.1 forcefield (Cornell, 1995). In the table are summarised the most important aspects of such simulation in the NVE ensemble for the DNA oligomer. During the acquisition a NVT ensemble can be sampled using a Nosé-Hoover thermostat. This has been done for the NK-2 homeodomain simulation. The MD setup and equilibration is similar for the two systems. The deterministic time evolution contained in the MD trajectory is never used in the diffusive method.

The trajectories, generated using this protocol applied to DNA oligomers in B canonical forms or to small proteins like the three-helix bundle NK-2 homeodomain, describe the statistical fluctuation of the molecules about given tertiary motives. Occasional slow conformational transitions occur within the ns time window, but they are not sampled properly to give their real influence onto the statistics. This information emerges from the analysis of averages and fluctuations of geometrical and order parameters (dihedral angles, mutual orientations). Therefore, through the diffusive equation we study the orientational dynamics of bonds (C—H or N—H, those involved in NMR relaxivities) as it is extracted by the statistics of stiff macromolecules fluctuating around defined structures.

5. RESULTS

We have applied the ORZLD and RM2-II approximation to the solution of the diffusion equation in order to compute the ^{13}C and ^{15}N nmr T_1

relaxation parameters respectively for the DNA d(TpCpGpCpG)$_2$ oligomer (Fausti, 1999) and the NK-2 homeodomain (La Penna, 1999; La Penna, 1999*), and compare them to experimental data (Borer, 1994; Gruschus, 1997).

5.1. DNA

In Figures 1, 2 and 3 we compare second order RM2-II ($e = 4$) and first order ORZLD T_1, for the model with finer beads, to the experimental data for $\nu(^1\text{H})$ equal to 250, 360 and 500 MHz respectively. The agreement is very good especially in the high frequency case. Even the ORZLD approximation gives good results considering the simplicity of the model. The low values for the C6 and C8 carbons are mainly due to the effect of chemical shift anisotropy even if they always show the larger correlation time within each nucleotide. The C5′ carbons show the highest mobility and the highest relaxation times that are related to the low correlation times. The carbon on the sugar rings show an intermediate range of relaxation parameters within each nucleotide, thus not allowing a discrimination between different atoms in the sugar ring. As expected T_1 and T_6 are more affected by fast motions since they are not stacked in base pairs, but on the other hand there are slow conformational transitions that are not completely sampled. Therefore, the agreement between computed and experimental results is better in the stiffer regions of the macromolecule. The same effects have been observed for proteins in the terminal regions or in the disordered loops (see later).

It is interesting to study the effect of the introduction of modes in the RM2-II approximations. In Figure 4 we show the comparison between the results obtained with $e = 3$, 4 and 5 at the highest frequency. The convergence seems to be good, even if the worth use of larger value for e is limited by the matrices diagonalisation. The application of a sorting procedure to limit the matrix dimensions is in progress.

5.2. NK-2

As far as the NK-2 homeodomain ^{15}N T_1 pattern is concerned, the diffusive method well describes the data of the lower frequency ($\nu(^1\text{H}) =$ 360 MHz) (Fig. 5, top). The agreement is better in the most rigid portion of the macromolecule (helix I), while, again, the spots in the calculated pattern are due to incomplete sampling of the conformational transitions in the flexible portion of the chain (head and tail, not structured in α helices).

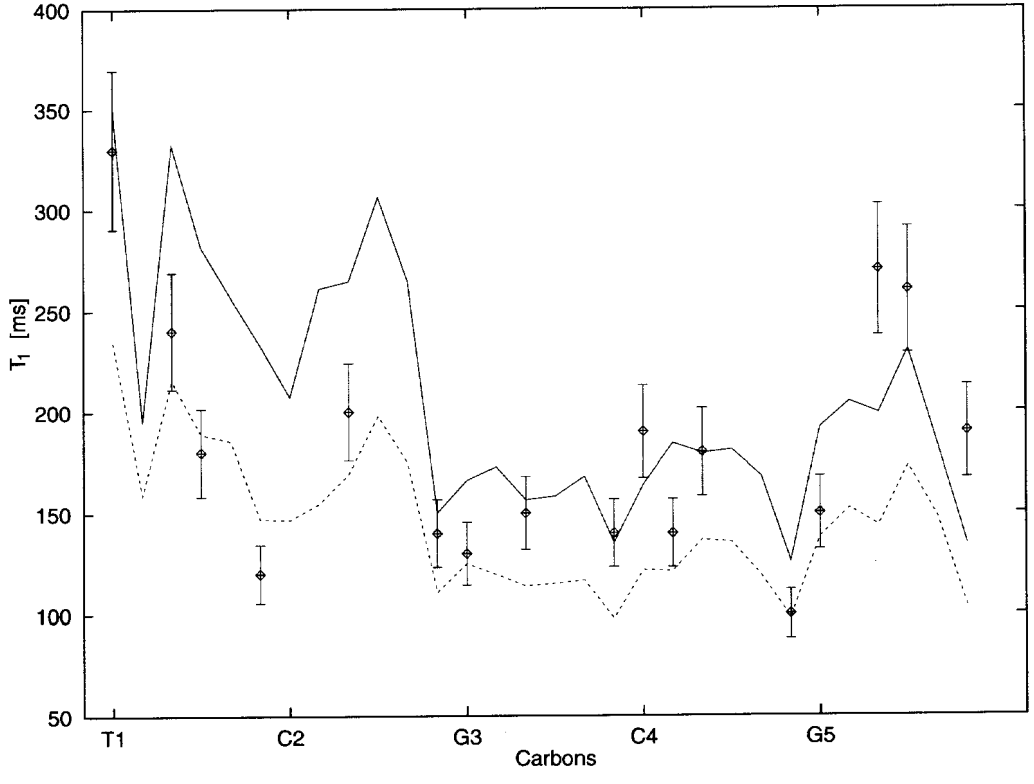

FIGURE 1 DNA oligomer ^{13}C relaxation times T_1 of different C nuclei at $\nu(^1H) = 250\,MHz$, using the finer bead model (SC): experimental data (points with error bars); ORZLD approximation (solid line); RM2-II ($e = 4$) model (dotted line). The sequence of carbon atoms is C5′, C4′, C3′, C2′, C1′ and C6 (T, C) or C8 (G).

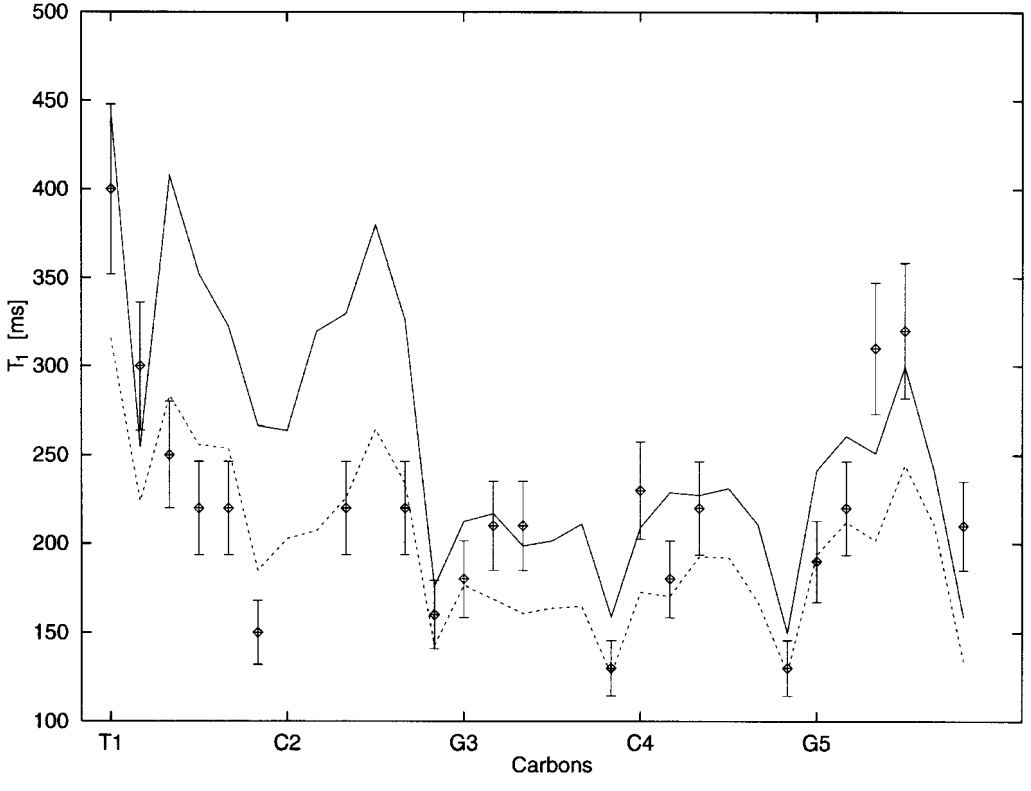

FIGURE 2 Same as in Figure 1 at $\nu(^1\mathrm{H}) = 360\,\mathrm{MHz}$.

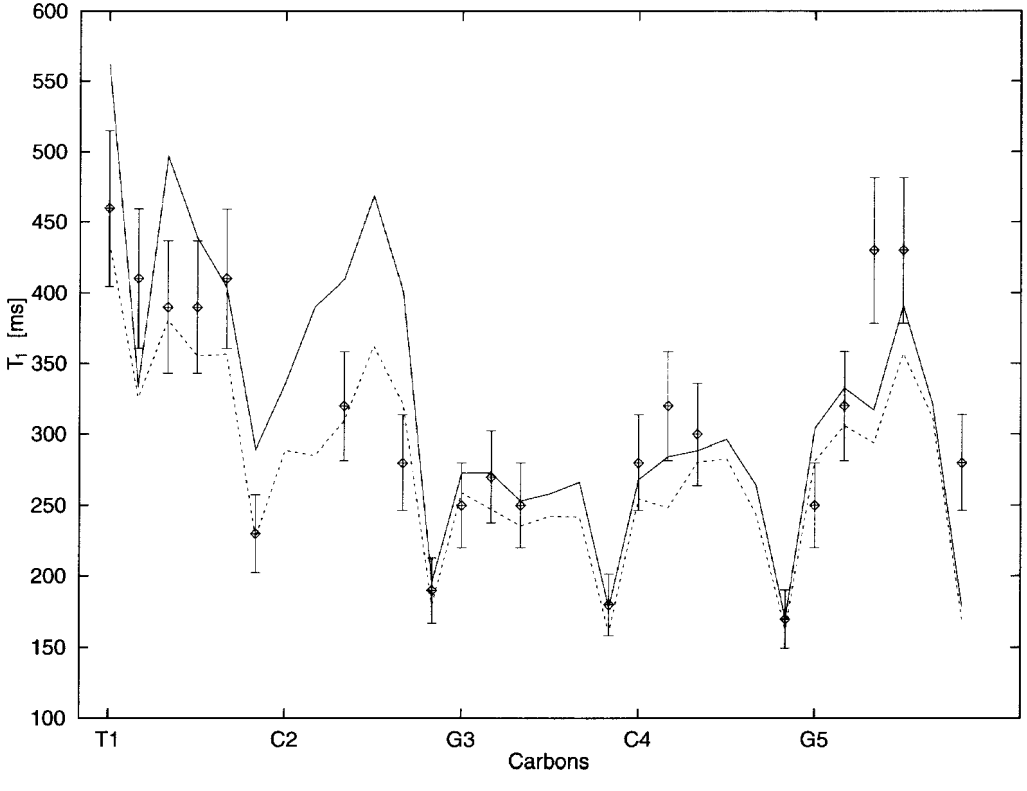

FIGURE 3 Same as in Figure 1 at $\nu(^1H) = 500\,MHz$.

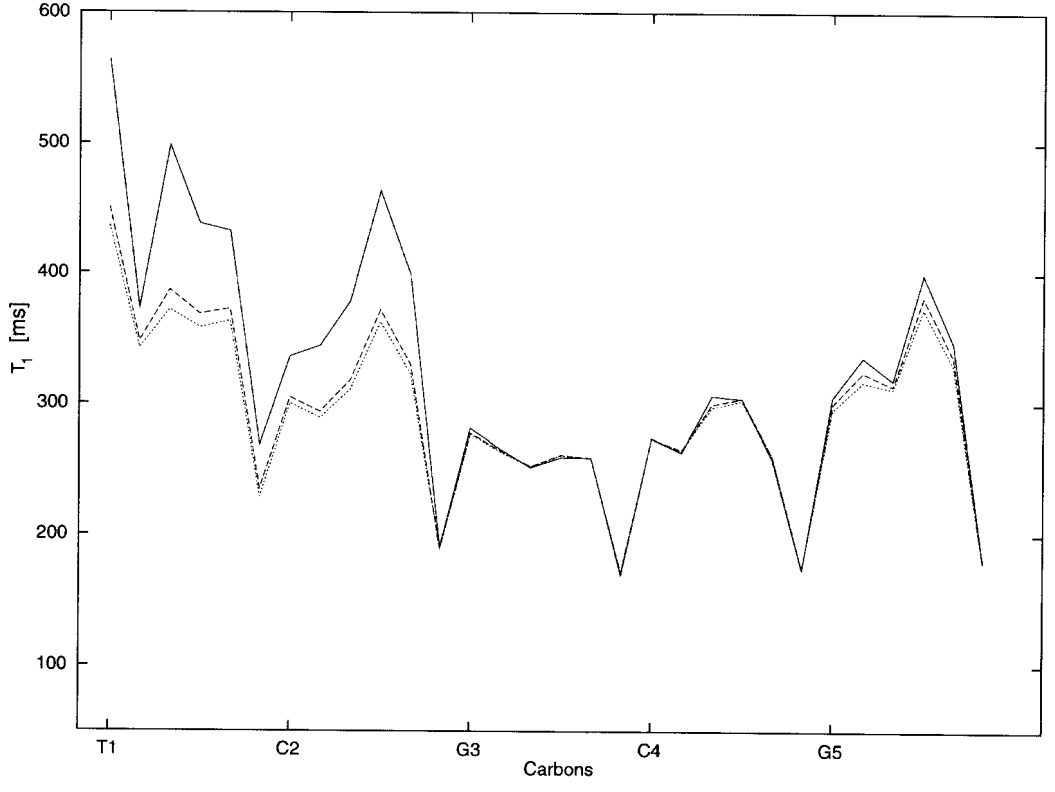

FIGURE 4 Same as in Figure 3 using a different number of modes e in the build-up of RM2-II basis sets: $e = 3$ (solid line); $e = 4$ (dashed line) and $e = 5$ (dotted line).

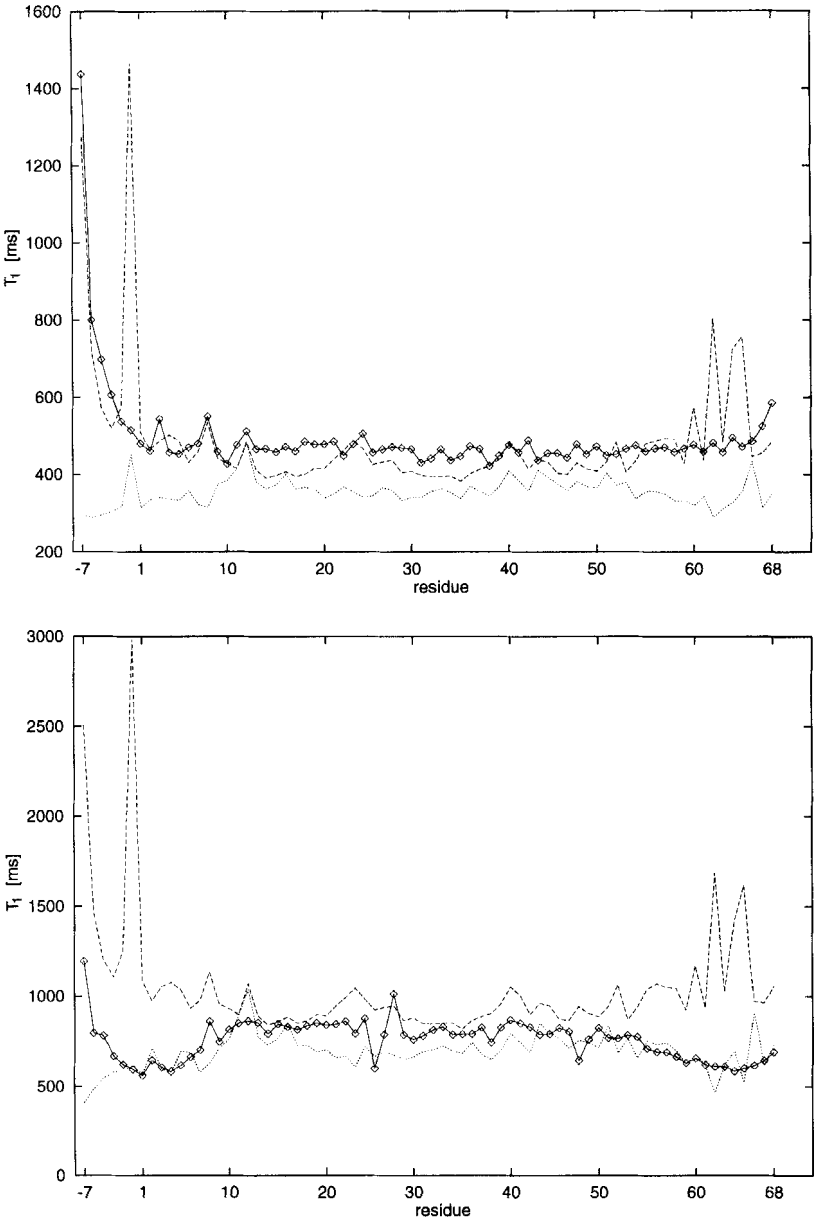

FIGURE 5 NK-2 ^{15}N relaxation times T_1 of amide N nuclei in the backbone at $\nu(^1H)$ = 360 MHz (top) and $\nu(^1H)$ = 600 MHz (bottom) using the "virtual bond" bead model (one bead for each residue): experimental data (points with solid line); RM2-II (e = 3) approximation (dashed line); biexponential approximation for the P_2 time correlation function, with the fastest rates scaled by the factor 1/50 (dotted line).

The experimental relaxation data at higher frequency ($\nu(^1H) = 600\,MHz$) (Fig. 5, bottom) show an interesting feature due to the larger effects of the local dynamics in the flexible regions. The well in the 5–15 residues region, for instance, is not shown by the calculated RM2-II approximation (dashed line) that contains most of the rotational information (already present in the lower frequency case) in the relaxation. What is interesting is that the fluctuations of these terminal regions are not localised on single residues, but they are spread along at least ten residues. The relaxation modes responsible of such "well effect" at high frequency can be represented just scaling the faster "non rotational" rates, for instance by a factor 1/50 (dotted lines). This scaling makes the collective internal fluctuations of the terminal regions more efficient in the modification of the relaxation pattern at high frequency, something that is observed experimentally. This scaling correction shows that even if coupling the modes with lower rates we better describe the rotation, we neglect important part of the internal collective fluctuations. It is not clear, however, if a richer statistics would be able to better describe collective modes with higher rates, that seem to be important, even keeping the RM2-II approximation.

References

Abragam, A. (1986) *Principles of Nuclear Magnetism*, Clarendon Press, Oxford, U.K.

Bixon, M. and Zwanzig, R. (1978) *J. Chem. Phys.*, **68**, 1896–1902.

Borer, P. N., LaPlante, S. R., Kumar, A., Zanatta, N., Martin, A., Hakkinen, A. and Levy, G. C. (1994) *Biochemistry*, **33**, 2441–2450.

Chang, X. Y. and Freed, K. F. (1993) *J. Chem. Phys.*, **99**, 8016–8030.

Cornell, W. D., Cieplak, P., Bayly, C. I., Gould, I. R., Merz, K. M. Jr., Ferguson, D. M., Spellmeyer, D. C., Fox, T., Caldwell, J. W. and Kollman, P. A. (1995) *J. Am. Chem. Soc.*, **117**, 5179–5197.

Duane, S., Kennedy, A. D., Pendleton, B. J. and Roweth, D. (1987) *Phys. Lett. B*, **195**, 216.

Edward, J. T. (1970) *J. Chem. Educ.*, **47**, 261–269.

Essmann, U., Perera, L., Berkowitz, M. L., Darden, T., Lee, H. and Pedersen, G. L. (1995) *J. Chem. Phys.*, **103**, 8577–8593.

Ewald, P. P. (1921) *Ann. Phys.*, **64**, 253–287.

Fausti, S., La Penna, G., Cuniberti, C. and Perico, A. (1999) **50**, 613–629.

Favro, D. L. (1960) *Phys. Rev.*, **119**, 53–62.

Frenkel, D. and Smit, B. (1996) *Understanding Molecular Simulation*, Academic Press, San Diego, U.S.A.

Gaudin, F., Genest, D. and Lancelot, G. (1997) *Eur. Biophys. J.*, **26**, 239–245.

Gaudin, F., Chanteloup, L., Thuong, N. T. and Lancelot, G. (1997) *Magnetic Resonance in Chemistry*, **35**, 561–565.

Gaudio, A. C. and Takahata, Y. (1992) *Computers Chem.*, **16**, 277–284.

Hu, Y., Fleming, G. R., Freed, K. F. and Perico, A. (1991) *Chem. Phys.*, **158**, 395–408.

Hu, Y., Kostov, K., Perico, A., Smithline, S. and Freed, K. F. (1995) *J. Chem. Phys.*, **103**, 9091–9100.

Jorgensen, W. L., Chandrasekhar, J., Madura, J. D., Impey, R. W. and Klein, M. (1983) *J. Chem. Phys.*, **79**, 926–935.

Kostov, K. S., Freed, K. F. and Perico, A. (1993) *Biopolymers*, **33**, 1423–1429.
Kostov, K. S. and Freed, K. F. (1997) *J. Chem. Phys.*, **106**, 771–783.
Kostov, K. S., Freed, K. F., Webb III, E. B., Mondello, M. and Grest, G. S. (1998) *J. Chem. Phys.*, **108**, 9155–8167.
La Penna, G., Mormino, M., Pioli, F., Perico, A., Fioravanti, R., Gruschus, J. M. and Ferretti, J. A. (1999) *Biopolymers*, **49**, 235–254.
La Penna, G., Fausti, S., Perico, A. and Ferretti, J. A., *Biopolymers*, submitted.
La Penna, G., Pratolongo, R. and Perico, A. (1999) *Macromolecules*, **32**, 506–513.
Lipari, G. and Szabo, A. (1984) *J. Am. Chem. Soc.*, **104**, 4546–4559.
Martyna, G. J., Tobias, D. J. and Klein, M. L. (1994) *J. Chem. Phys.*, **105**, 4177–4189.
Mattice, W. L. and Suter, U. W. (1994) *Conformational theory of large molecules*, John Wiley & Sons, New York, U.S.A.
Pastor, R. W. and Karplus, M. (1988) *J. Phys. Chem.*, **92**, 2636–2641.
Pearlman, D. A., Case, D. A., Caldwell, J. W., Ross, W. S., Cheatham III, T. E., DeBolt, S., Ferguson, D. M., Seibel, G. and Kollman, P. A. (1995) *Comput. Phys. Commun.*, **91**, 1.
Pearlman, D. A., Case, D. A., Caldwell, J. W., Ross, W. S., Cheatham III, T. E., DeBolt, S., Ferguson, D. M., Seibel, G. and Kollman, P. A. (1995) Amber 4.1, University of California, San Francisco, U.S.A.
Perico, A. and Pratolongo, R. (1997) *Macromolecules*, **30**, 5958–5969.
Perico, A. and Guenza, M. (1985) *J. Chem. Phys.*, **83**, 3103–3109.
Perico, A. (1989) *Accounts Chem. Res.*, **22**, 336–342.
Perico, A., Guenza, M., Mormino, M. and Fioravanti, R. (1995) *Biopolymers*, **35**, 47–54.
Perico, A., Piaggio, P. and Cuniberti, C. (1975) *J. Chem. Phys.*, **62**, 4911–4918.
Perico, A., Pratolongo, R., Freed, K. F. and Szabo, A. (1994) *J. Chem. Phys.*, **101**, 2554–2561.
Perico, A., Pratolongo, R., Freed, K. F., Pastor, R. W. and Szabo, A. (1993) *J. Chem. Phys.*, **98**, 564–573.
Procacci, P., Darden, T. and Marchi, M. (1996) *J. Phys. Chem.*, **100**, 10464–10468.
Procacci, P., Paci, E., Darden, T. and Marchi, M. (1996) *J. Comp. Chemistry*, **18**, 1848–1862.
Rose, M. E. (1957) *Elementary Theory of Angular Momentum*, John Wiley & Sons, New York, U.S.A.
Saenger, W. (1984) *Principles of Nucleic Acid Structure*, Springer-Verlag, New York, U.S.A.
Tang, W. H., Chang, X. Y. and Freed, K. F. (1995) *J. Chem. Phys.*, **103**, 9492–9501.
Tuckerman, M., Berne, B. J. and Martyna, G. J. (1992) *J. Chem. Phys.*, **97**, 1990–2001.
Zhou, R. and Berne, B. J. (1997) *J. Chem. Phys.*, **107**, 9185–9196.